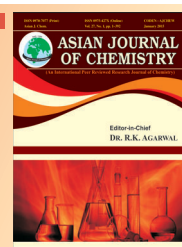




Asian Journal of Chemistry; Vol. 27, No. 4 (2015), 1411-1416

# ASIAN JOURNAL OF CHEMISTRY

<http://dx.doi.org/10.14233/ajchem.2015.18061>



## Thermal and Spectroscopic Dynamics of Titanium Oxide Functionalized Polyaniline Coated Sawdust

MANGAKA MATOETOE\*, FREDRICK OKUMU, CONNIE MAPHALE and OLALEKAN FATOKI

Department of Chemistry, Cape Peninsula University of Technology, P.O. Box 652, Cape Town 8000, South Africa

\*Corresponding author: Fax: +27 21 4603854; Tel: +27 21 4603163; E-mail: lellangm@gmail.com

Received: 22 May 2014;

Accepted: 1 September 2014;

Published online: 4 February 2015;

AJC-16803

Natural cellulose (sawdust) usage is limited by its poor physical and chemical properties. This study looks into the effects of chemical treatment of sawdust with polyaniline. Polyaniline (PANI) was chemically polymerized *in situ* from aniline in acid medium containing sawdust and/or titanium oxide (TiO<sub>2</sub>) to form polyaniline composites (PANI/SD, PANI/SD/TiO<sub>2</sub> and PANI/SD/TiO<sub>2</sub>). These composites spectrophotometric, structural, morphological and thermal properties were determined using various spectrophotometric techniques such as fourier transform infrared (FTIR), UV-visible, transmission electron microscope (TEM), thermogravimetric (TG) and differential scanning calorimetry (DSC) and powder X-ray diffraction (PXRD). Results indicate structure retention by the polyaniline, Sawdust and titanium oxide. However, minor chemical shifts were indicative of a physio-chemical interaction between the functional groups. The marked morphological changes observed from the pure chemicals and composites suggests multi-layer formation. Thermal studies showed two weight loss waves; 1<sup>st</sup> waves are due to water and doping material loss while 2<sup>nd</sup> wave losses are a result of polymer decomposition. The weight loss trend was: PANI/SD < PANI < PANI/SD/TiO<sub>2</sub> < PANI/TiO<sub>2</sub>, thus suggesting a thermal stability improvement with the addition of TiO<sub>2</sub>. Powder X-ray diffraction confirmed the structural retention of pure polyaniline and sawdust as indicated by the appearance of their representative broad 2θ angles at 20°, 26° and 15°, 24°.

**Keywords:** Polyaniline, Composite, Sawdust, Titanium oxide.

### INTRODUCTION

The natural cellulosic materials are abundant, renewable, low cost and of low density. Therefore, their composites are cost effective and environmentally friendly. However, lack of consistent quality, interfacial adhesion and poor resistance to moisture absorption makes the use of natural fibers less attractive for critical applications. These problems have been successfully alleviated by suitable chemical treatments. It is well known that natural fibers can be used in synthesis of composites. Several composites such as nanoclay/natural cellulose (fiber) and organic polymer/cellulose or fibers have been reported<sup>1</sup>. These composites are reported as stable, reinforced and tailor made for the intended usage. As a result of the reinforcement of the final product the fibers have commonly been used as fillers in packaging and construction as well as adsorbent materials in waste water remediation<sup>1</sup>. Thus, development and progression of these natural cellulose polymer materials will improve waste disposal and lead to economic development in most countries that have large quantities of these cellulosic waste<sup>2</sup>.

Among the polymers that have been used, polyanilines are the commonest. Polyaniline (PANI) family has been of much interest in composites because of their diverse structures, special doping mechanism, excellent environmental stability, good solution processability and high conductivity. Additionally, they have interesting properties such as chemical sensitivity and multicolour electrochromism which are essential characteristics required for electronic devices<sup>3</sup>. These materials offer wide applicability in technological fields, such as electronic and electrochromic devices<sup>4</sup>, chemical sensors<sup>5</sup>, charge storage systems<sup>6</sup> and the protection against corrosion<sup>7</sup>. Composites made up of polyaniline and inorganic materials and organic such as PVS<sup>8</sup> have been reported. Hybrid such as PANI/WO<sub>3</sub><sup>9</sup>, PANI/Co<sub>3</sub>O<sub>4</sub><sup>10</sup> and PANI/CeO<sub>2</sub><sup>11</sup> and their applications for the humidity sensing properties have been studied. Other literature reports are on a variety of nanohybrids such as PANI-MoO<sub>3</sub><sup>12</sup>, PANI-V<sub>2</sub>O<sub>5</sub><sup>13</sup>, PANI-Fe<sub>2</sub>O<sub>3</sub><sup>14</sup> and PANI-SnO<sub>2</sub><sup>15</sup> which have been investigated for different purposes. In recent years composites made from natural (cellulosic) waste materials and organic polymers have gained a lot of interest in construction automobile industry and remediation<sup>16,17</sup>.

Polyaniline and sawdust (PANI/SD) composites usage as an adsorbent for metals (lead, chromium) and organic compounds (dyes, polychlorinated biphenyls) have been reported<sup>16-18</sup>. However, the interrogation of the adsorbent is lacking especially the morphology and thermal properties of these hybrids. In the present work chemical synthesis and interrogation of the polyaniline, TiO<sub>2</sub> and sawdust (SD) composites by spectroscopic techniques is reported. This involved morphological characterization such as size and shape of the composites formed, degree of dispersion, kind of interaction and interface between the compounds in the composites. The study involved comparison of the spectra of the composites with the spectra of pure compounds which are components of the composites. Understanding of the dynamics of the composites is vital in applications of the materials. Therefore the knowledge from the study will enable design and widespread usage of the polyaniline composites.

## EXPERIMENTAL

The reagents used in this study included aniline (99 % purity, Sigma Aldrich) which was doubly-distilled before use under reduced pressure and stored at a low temperature, hydrochloric acid (37 %), analytical grade ammonium persulfate (APS), sawdust in the form of fine particles were used directly without additional treatment. N,N-dimethyl formamide, (DMF) (anhydrous, 99.8 %, Analytical grade), titanium dioxide (TiO<sub>2</sub>) from fluka analytical. Deionized water was used for aqueous solution preparations.

**Synthesis of polyaniline composites:** Polyaniline was synthesized from 0.02 M aniline in 1 M HCl and stirred continuously. Then 2.5 g of ammonium persulfate was added to the solution mixture with continuous stirring. The mixture was allowed to polymerize at room temperature for 24 h. The precipitate formed was collected by filtering on a Buchner funnel using a water aspirator and washed with distilled water then left to dry at room temperature. For PANI/SD composite, accurately weight amount of sawdust was first soaked in 1 M HCl and then aniline was added to the mixture. Finally 2.5 g of ammonium persulfate was added to the mixture and stirred continuously for 24 h at room temperature while polymerization occurred. The composites were then removed from the solution, washed thoroughly in distilled water to remove traces of monomers and HCl and in a dry place. For PANI/TiO<sub>2</sub> synthesis, TiO<sub>2</sub> particles were added to the mixture containing

ammonium persulfate, aniline and HCl before polymerization occurred. Similarly for PANI/SD/TiO<sub>2</sub> synthesis, sawdust was first soaked in acid and TiO<sub>2</sub> added to the mixture containing ammonium persulfate, aniline and HCl<sup>18-20</sup>.

**Characterization of the composites:** The FTIR spectra of the polyaniline and its composite were recorded using Perkin Elmer model Spectrum 100 series in the range of 4000-400 cm<sup>-1</sup> at room temperature. UV-visible spectra were recorded in the 250-800 nm range using a 1 cm path length quartz cuvette and pure DMF was used as the reference on a Nicolet evolution 100 spectrophotometer. The powder X-ray diffraction (PXRD) was performed by using a Bruker AXS D8 advance diffractometer. The studies on the morphology and size distribution of the polyaniline composite were performed by using a high resolution transmission electron microscope (HRTEM) from Tecnai G2F20 X-Twin MAT (US) and the SEM images taken using a JEOL JSM-7500F scanning electron microscope. The amount of weight loss and the thermostability of polyaniline and its composite were determined from thermogravimetric analysis (TGA). Both thermogravimetric analysis (TG) and differential scanning calorimetry (DSC) were performed on a Perkin Elmer Pyris 6 system was used for thermogravimetric measurements of the samples from 30 to 400 °C in air at the heating rate of 10 °C/min. The weight of the sample used was 3 mg in all cases.

## RESULTS AND DISCUSSION

The synthesis and different oxidation states of polyaniline are well documented<sup>18</sup>. In the leucomeraldine base (LB), polyaniline existed in a reduced state with pale yellow appearance which transformed to green in pernigraniline oxidized base (POB) and appears dark green in the neutral emeraldine base (EB). Further oxidation resulted in the pernigraniline base (PB) state which corresponds to the purple appearance. The green coloured neat polyaniline obtained (Fig. 1) is indicative of emeraldine redox state<sup>19</sup>. Emeraldine base is normally regarded as the most useful form of polyaniline due to its high stability at room temperature and the fact that, upon doping with acid, the resulting emeraldine salt form of polyaniline is highly electrically conducting<sup>21</sup>.

The UV-visible and FTIR spectrophotometry data of the composites is tabulated in Table-1. The characteristic peaks due to C-N stretch aromatic indicative of the nitrogen bonded benzene (N=B=N) and quinoid (N=Q=N) rings were observed



Fig. 1. Appearance of the polyaniline composites synthesized; SD (light brown), polyaniline (PANI) (dark green), PANI/SD (brown), PANI/TiO<sub>2</sub> (light green) and PANI/SD/TiO<sub>2</sub> (light green) after synthesis

TABLE-1  
CHARACTERISTIC FTIR BAND FREQUENCIES AND UV VISIBLE ABSORPTION

Hybrids	FTIR band frequencies (cm <sup>-1</sup> )					UV-visible $\lambda_{\max}$ (nm)	
	C-H bending (830)	C-N stretching (Aromatic) (1121)	C-N stretching (1295)	Aromatic N=C=N (Benzenoid) (1489)	Aromatic N=Q=N (Quinoid) (1577)	$\pi$ - $\pi^*$ Benzenoid (327-365)	n- $\pi^*$ Quinine-imine (600-620)
PANI	805	1193	1280	1400	1500	367	598
PANI/SD	807	1210	1290	1400	1500	321	617
PANI/TiO <sub>2</sub>	818	1197	1296	1401	1500	330	630
PANI/SD/TiO <sub>2</sub>	817	1198	1297	1401	1500	322	618

around 1400 and 1500 cm<sup>-1</sup>, respectively for both polyaniline and hybrids. This suggests that they are no structural differences between the isolated polyaniline and polyaniline in the composites. The bands around 805, 1193 and 1280 cm<sup>-1</sup> in polyaniline and its composites are due to C-H out of plane bending, C-N stretching in aromatic and non-aromatic, respectively. In composites, these groups' vibrational frequencies showed a shift towards higher wave number as compared to isolated polyaniline value which indicated the presence of physiochemical bonding between polyaniline and titanium oxide/sawdust. Similar results have been reported elsewhere<sup>17</sup>.

The UV-visible spectra data (Table-1) indicates presence of two distinct peaks around 327-365 and 600-620 nm regions due to  $\pi$ - $\pi^*$  (benzenoid) and n- $\pi^*$  (quinine-imine) transitions in both polyaniline and composites. This confirms that polyaniline backbone is intact in the composites. However, the composites wavelength further showed a blue shift at the lower wavelength (300 nm) while a red shift was observed at the higher wavelength region (600 nm). Thus collaborating IR data, regarding presence of physiochemical bonding between polyaniline and the titanium oxide/sawdust at both the quinoid and benzenoid sites<sup>18</sup>.

**Morphological characterization:** Morphological studies of the composites were studied using scanning electron microscopy (SEM) and transmission electron microscopy (TEM). Fig. 2a to 2d show the SEM images of polyaniline, sawdust, PANI/SD, PANI/TiO<sub>2</sub> and PANI/SD//TiO<sub>2</sub>, respectively at a magnification of 100  $\mu$ m. Visual inspection of SEM microgram show various morphological appearance depending on the components of the composite, all the powders have rough surfaces. Polyaniline powder (Fig. 2a) appears to have numerous honeycombed structures with observable pores within the polymer matrix as reported by Chao and co-workers<sup>22</sup>. The sawdust (Fig. 2b) depicts regular network pattern which disappeared in the subsequent composite formations, while the PANI/SD (Fig. 2c) had aligned rod-like structures with uniform distribution of sawdust particles in the polyaniline matrices, showing no apparent aggregations. This indicates possible strong interactions between polymer molecules and sawdust particles. PANI/TiO<sub>2</sub> composite particles (Fig. 2d) and PANI/SD/TiO<sub>2</sub> (Fig. 2e) had cauliflower shapes which were highly dispersed with dark spheres of TiO<sub>2</sub> aggregated. The similarities in the micrograph indicates preservation of the composites components, thus suggesting van der Waals interaction between polymer molecules and the other components of the composite (SD and TiO<sub>2</sub>) or interactions due to charge transfer from the nitrogen atom of the quinoid units of the polymer to sawdust and TiO<sub>2</sub> particles<sup>23</sup>.

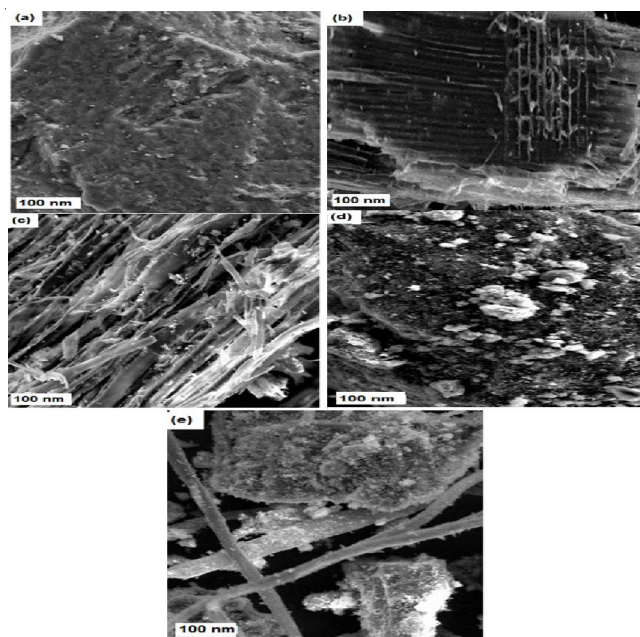


Fig. 2. SEM micrographs of (a) polyaniline (b) acid treated SD (c) PANI/SD, (d) PANI/TiO<sub>2</sub> and (e) PANI/SD/TiO<sub>2</sub> with a magnification of 100  $\mu$ m

The TEM micrograms of polyaniline, sawdust, PANI/SD, PANI/TiO<sub>2</sub> and PANI/SD/TiO<sub>2</sub> were depicted in Fig. 3a-e, respectively had rods like (Fig. 3a, b and e) and spherical shapes (Fig. 3c and d). The rod are arranged as a neat network, clusters and aggregates for Fig. 3a, b and (e), respectively while the spherical shapes observed in Fig. 3c were larger compared to PANI/TiO<sub>2</sub>. In both PANI/SD and PANI/TiO<sub>2</sub> (Fig. 3c and d), the distribution of particles sizes observed was approximately 30 nm. It was possible that these large particles were aggregates of smaller particles that coagulated together during the drying of dispersions for TEM. The micrographs showed that the presence of TiO<sub>2</sub> and sawdust particles caused changes in morphology of the polyaniline in the respective composite. In both cases, the products appeared to be composed of highly amorphous particles with high surface area. The TEM image of the PANI/SD/TiO<sub>2</sub> composite in Fig. 3e showed smeared dark spheres due to the doped polyaniline, which was similarly reported by Wei *et al.*<sup>24</sup>. It was observed that TiO<sub>2</sub> and polyaniline were well dispersed in the composite and the surfaces of the PANI/TiO<sub>2</sub> composite were strongly affected by the TiO<sub>2</sub> aerogel structure and therefore modified the morphology of polyaniline significantly. The surfaces of the PANI/SD/TiO<sub>2</sub> composite particles were different from those of the pure polyaniline due to the interpenetration of polyaniline in TiO<sub>2</sub> structure as shown in Fig. 3e. The resultant PANI/SD/TiO<sub>2</sub> material

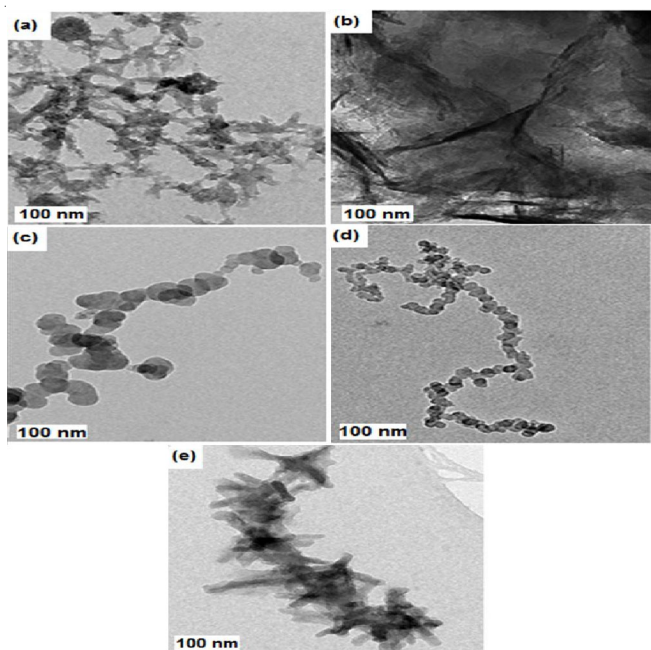


Fig. 3. TEM microgram of (a) pure polyaniline (b) acid treated SD, (c) PANI/SD (d) PANI/TiO<sub>2</sub> and (e) PANI/SD/TiO<sub>2</sub> particles. Micrographs obtained at 100 keV with a magnification of 100 nm

therefore showed well dispersed particles of sawdust and TiO<sub>2</sub> around the polyaniline backbone structure. The addition of TiO<sub>2</sub> resulted in reduced particle size of the composite leading to changes in morphological structure of heaped composite from loose cotton to firm gravel in appearance which showed that the TiO<sub>2</sub> particles had a nucleation effect on the polymerization, leading to a homogeneous polyaniline shell around them<sup>25</sup>.

**Thermal analysis:** It has been found that the chemical composition, chemical properties, morphological and physical properties of polyaniline composite depend on the type of dopant, medium and interaction of polyaniline and dopant<sup>26</sup>. The TG-DSC curves of the polyanilines were shown in Fig. 4a-d. All the polyanilines had a two-step mass loss processes which were similar to other observations<sup>27,28</sup>. The onset of the decomposition for the thermogram was 150 °C with most weight losses occurring between 160 and 400 °C. The first weight loss around 60 to 140 °C was attributed to the expulsion of water and dopant components (sawdust and TiO<sub>2</sub>) from the polyaniline matrix. The second step involved mass loss initiation between 160 and 400 °C varied depending on the composite. This step was due to the degradation of the polyaniline backbone. In the composites, the onset of degradation occurred at

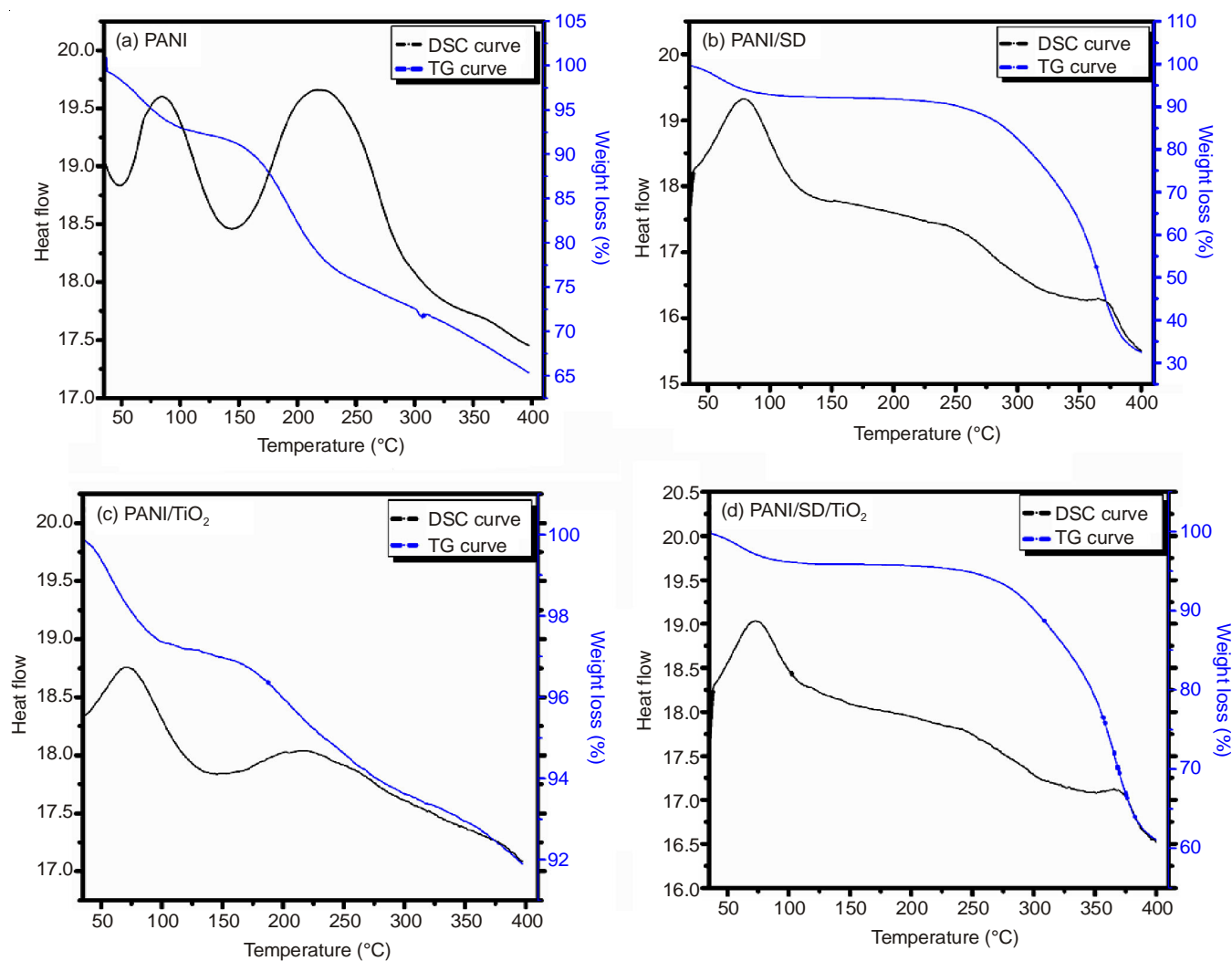


Fig. 4. TGA curves and corresponding DSC curves for pure polyaniline and its composites (a) PANI, (b) PANI/SD, (c) PANI/TiO<sub>2</sub> and (d) PANI/SD/TiO<sub>2</sub>

20 °C lower than that of pure polyaniline, suggesting that the composite influences the structure and thermal stability of polyaniline<sup>29</sup>. The onset of the decomposition of polyaniline and PANI/SD were 150 and 260 °C, respectively while that for PANI/TiO<sub>2</sub> and PANI/SD/TiO<sub>2</sub> were 260 °C in each case. The thermal stability comparison of the polyaniline composite showed an increasing trend from PANI/SD < PANI/SD/TiO<sub>2</sub> < PANI/TiO<sub>2</sub> composite (Fig. 4). The difference in temperature can be explained by the strong interaction between TiO<sub>2</sub> and polyaniline due to the interpenetrating structure of the PANI/TiO<sub>2</sub> composite particles. The DSC curves of polyanilines (Fig. 4) show that the polyaniline and its composite under nitrogen atmosphere displayed endothermic peaks. In all these curves, endothermic peaks were observed at lower temperatures of 85 °C (PANI), 77 °C (PANI/SD), 67 °C and 72 °C (PANI/SD/TiO<sub>2</sub>) and were ascribed to the loss of water or release of moisture content and other combined small molecules<sup>30</sup>, which was consistent with the thermogravimetric analysis result. The second thermal event was related to the decomposition of amine units of the polyaniline molecules with corresponding endothermic peaks at 219 °C (PANI), 325 °C (PANI/SD), as similarly discussed<sup>31</sup>. This was also associated with a considerable weight loss in thermogravimetric analysis measurement. In the case of PANI/TiO<sub>2</sub> and PANI/SD/TiO<sub>2</sub> the second peak were observed at 225 and 375 °C, respectively (Fig. 4). This could be due to the strong interaction between TiO<sub>2</sub> and polyaniline due to the interpenetrating structure of the PANI/TiO<sub>2</sub> and PANI/SD/TiO<sub>2</sub> composite particles.

**Powder X-ray diffraction patterns:** The powder XRD patterns of sawdust, polyaniline and its composite are illustrated in Fig. 5. Pure polyaniline powder (a) exhibited two broad peaks at 2θ angles of 20° and 26°, which may be assigned to the scattering from polyaniline chains at interplanar spacing<sup>32</sup>. The polyaniline characteristic peak at 26° was associated with the amorphous structure of polyaniline<sup>33</sup>. In the diffraction patterns of acid treated sawdust and PANI/SD, additional broad diffraction peaks were observed both at around 15° and 24° while the PXRD pattern of the PANI/TiO<sub>2</sub> and PANI/SD/TiO<sub>2</sub> composite powder (Fig. 5e), major diffraction peaks were observed at 11°, 37°, 47°, 53°, 61°, 68° and 75° which were attributed to the presence of TiO<sub>2</sub> phase<sup>29</sup>. PANI/SD/TiO<sub>2</sub> composite particles also had similar peaks with an additional peak at 24° indicative of the preserved backbone structure of PANI. The interpenetration of polyaniline into the TiO<sub>2</sub> network helped in the enhancement of the degree of crystallinity of PANI/TiO<sub>2</sub>. From the PANI/TiO<sub>2</sub> patterns in Fig. 5d, a strong narrow diffraction peaks were observed at 2θ 26°, thus suggesting enhanced crystallinity for the composite containing TiO<sub>2</sub> and not decreased crystallinity as reported by Xia and Wang<sup>34</sup>. In PANI/SD/TiO<sub>2</sub> patterns, the diffraction at 26° was narrow and strong compared to pure polyaniline (a) which was broad and weak. However, the effects of sawdust and TiO<sub>2</sub> in the PANI/SD/TiO<sub>2</sub> composite with TiO<sub>2</sub> might have been more predominant than sawdust causing the material to be crystalline. This was confirmed by the transformation of the amorphous structure of polyaniline to crystalline PANI/TiO<sub>2</sub> and PANI/SD/TiO<sub>2</sub> while a distortion in crystal structure of polyaniline was evident due to inclusion of sawdust during the polymerization reaction leading to transformation of the polyaniline into a more amorphous phase PANI/SD.

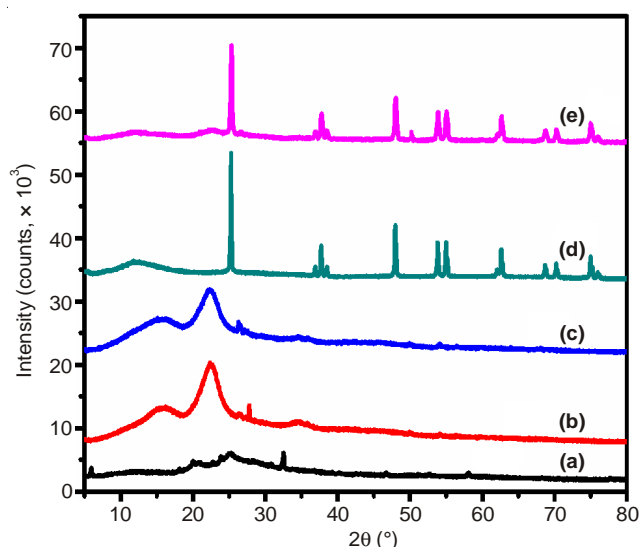


Fig. 5. Powder X-ray diffraction patterns of acid treated (a) polyaniline, (b) SD, (c) PANI/SD, (d) PANI/TiO<sub>2</sub> and (e) PANI/SD/TiO<sub>2</sub> composite

## Conclusion

Polyaniline composites were successfully synthesized through *in situ* polymerization. UV-visible spectra revealed that the polymers exhibited two absorption bands corresponding to the two types of chemically non-equivalent rings in the polymer chain, benzenoid and quinoid groups, respectively. The FTIR spectra of polyaniline composite showed characteristic polyaniline peaks with the polyaniline composite peaks showing increased intensity as a result of close proximity of sawdust and TiO<sub>2</sub> at nitrogen sites to the aromatic hydrogens.

The formation of polyaniline composite distorted the polyaniline chains structure. The thermogravimetric analysis data suggested that polyaniline composite were more thermally stable than neat polyaniline due to the presence of sawdust and TiO<sub>2</sub> particles at the nitrogen sites that enhanced the thermal stability in the composite with PANI/TiO<sub>2</sub> and PANI/SD/TiO<sub>2</sub> being more stable to heat due to contribution from sawdust and TiO<sub>2</sub> particles in the final structure. Further studies showed that the thermal stability increased in the order of PANI < PANI/SD < PANI/SD/TiO<sub>2</sub> < PANI/TiO<sub>2</sub>. The SEM micrographs of the neat polyaniline revealed homogenous distribution of sawdust and TiO<sub>2</sub> in polyaniline matrix. Polyaniline and its composite exhibited pore like structures indicating good porosity that may be useful in applications as adsorbent materials. Similar outcome for TEM results showed that all the materials synthesized varied depending on the evidence that the PANI/SD/TiO<sub>2</sub> were well dispersed with structures showing the pores. The powder X-ray diffraction showed the composites were mostly amorphous with few crystalline exceptions and the neat polyaniline structure was retained in each composite with confirmation of the presence of sawdust and TiO<sub>2</sub> phase in the composite.

## ACKNOWLEDGEMENTS

The authors are grateful to Cape Peninsula University of Technology for funding and support

## REFERENCES

1. K. Majeed, M. Jawaid, A. Hassan, A.H.P.S. Abu Bakar, H.P.S. Abdul Khalil, A.A. Salema and I. Inuwa, *Mater. Des.*, **46**, 391 (2013).
2. R. Gangopadhyay and A. De, *Chem. Mater.*, **12**, 608 (2000).
3. W.S. Huang and A.G. MacDiarmid, *Polymer*, **34**, 1833 (1993).
4. T. Kobayashi, H. Yoneyama and H.J. Tamura, *J. Electroanal. Chem.*, **161**, 419 (1984).
5. M.V. Deshpande and D.P. Amalnerkar, *Prog. Polym. Sci.*, **18**, 623 (1993).
6. A.G. MacDiarmid, S.L. Mu, N.L. Somasiri and W. Wu, *Mol. Cryst. Liq. Cryst.*, **121**, 187 (1985).
7. R. Noufi, A.J. Nozik, J. White and L.F. Warren, *J. Electrochem. Soc.*, **129**, 2261 (1982).
8. G. Neetika, D. Kumar and S.K. Tomar, *J. Mater. Chem.*, **2**, 79 (2012).
9. N. Parvatikar, S. Jain, S. Khasim, M. Revansiddappa, S.V. Bhoraskar and M.V.N.A. Prasad, *Sens. Actuators B*, **114**, 599 (2006).
10. N. Parvatikar, S. Jain, S.V. Bhoraskar and M.V.N. Ambika Prasad, *J. Appl. Polym. Sci.*, **102**, 5533 (2006).
11. N. Parvatikar, S. Jain, C.M. Kanamadi, B.K. Chougule, S.V. Bhoraskar and A.M.V.N. Prasad, *J. Appl. Polym. Sci.*, **103**, 653 (2007).
12. T.A. Kerr, H. Wu and L.F. Nazar, *Chem. Mater.*, **8**, 2005 (1996).
13. M.G. Kanatzidis, C.G. Wu, H.O. Marcy and C.R. Kannewurf, *J. Am. Chem. Soc.*, **111**, 4139 (1989).
14. M. Wan, W.X. Zhou and J.C. Li, *Synth. Mater.*, **78**, 27 (1996).
15. C. Dearmitt and S.P. Armes, *Langmuir*, **9**, 652 (1993).
16. R. Ansari and F. Raofie, *E-J. Chem.*, **3**, 35 (2006).
17. F. Kanwal, R. Rehman, T. Mahmud, J. Anwar and R. Ilyas, *J. Chil. Chem. Soc.*, **57**, 1058 (2012).
18. F. Okumu, M. Matoetoe and O. Fatoki, *Sci. J. Chem.*, **1**, 29 (2013).
19. T.T. Waryo, E.A. Songa, M.C. Matoetoe, R.F. Ngece, P.M. Ndagili, A. Al-Ahmed, N.M. Jahed, P.G.L. Baker and E.I. Iwuoha, in eds.: U. Yogeswaran, S.A. Kumar and S.-M. Chen; *Nanostructured Materials for Electrochemical Biosensors in Nanotechnology Science and Technology Series*, Nova, New York, pp. 39-64 (2009).
20. A.G. MacDiarmid, *Angew. Chem. Int. Ed.*, **40**, 2581 (2001).
21. G.G. Wallace, G.M. Spinks, L.A.P. Kane-Maguire and P.R. Teasdale, *Conductive Electroactive Polymers: Intelligent Materials Systems*, edn 2, CRC Press, Boca Raton, FL (2003).
22. D. Chao, J. Chen, X. Lu, L. Chen, W. Zhang and Y. Wei, *Synth. Met.*, **150**, 47 (2005).
23. H. Zengin and G. Kalayci, *Mater. Chem. Phys.*, **120**, 46 (2010).
24. C. Wei, Y. Zhu, X. Yang and C. Li, *Mater. Sci. Eng. B*, **137**, 213 (2007).
25. M.A. Salem, A.F. Al-Ghonemiy and A.B. Zaki, *Appl. Catal. B*, **91**, 59 (2009).
26. A.K. Cuentas-Gallegos and P. Gómez-Romero, *J. Power Sources*, **161**, 580 (2006).
27. M.C. Gupta and S.S. Umare, *Macromolecules*, **25**, 138 (1992).
28. S.H. Khor, K.G. Neoh and E.T. Kang, *J. Appl. Polym. Sci.*, **40**, 2015 (1990).
29. S. Wang, Z. Tan, Y. Li, L. Sun and T. Zhang, *Thermochim. Acta*, **441**, 191 (2006).
30. M. Ghorbani and H. Eisazadeh, *Synth. Met.*, **162**, 527 (2012).
31. F.S. Kittur, K.V. Harish Prashanth, K. Udaya Sankar and R.N. Tharanathan, *Carbohydr. Polym.*, **49**, 185 (2002).
32. W. Feng, E. Sun, A. Fujii, H. Wu, K. Niihara and K. Yoshino, *Bull. Chem. Soc. Jpn.*, **73**, 2627 (2000).
33. Z. Zhang, Z. Wei and M. Wan, *Macromolecules*, **35**, 5937 (2002).
34. H. Xia and Q. Wang, *Chem. Mater.*, **14**, 2158 (2002).